Cellular and Molecular Life Sciences (2022) 79:616
https://doi.org/10.1007/s00018-022-04643-1

ORIGINAL ARTICLE

Neutrophils play a major role in the destruction of the olfactory epithelium during SARS-CoV-2 infection in hamsters

Clara Bourgon[1] · Audrey St Albin[1] · Ophélie Ando-Grard[1] · Bruno Da Costa[1] · Roxane Domain[2] · Brice Korkmaz[2] · Bernard Klonjkowski[3] · Sophie Le Poder[3] · Nicolas Meunier[1]

Received: 8 June 2022 / Revised: 2 November 2022 / Accepted: 22 November 2022 / Published online: 3 December 2022

Abstract

The loss of smell (anosmia) related to SARS-CoV-2 infection is one of the most common symptoms of COVID-19. Olfaction starts in the olfactory epithelium mainly composed of olfactory sensory neurons surrounded by supporting cells called sustentacular cells. It is now clear that the loss of smell is related to the massive infection by SARS-CoV-2 of the sustentacular cells in the olfactory epithelium leading to its desquamation. However, the molecular mechanism behind the destabilization of the olfactory epithelium is less clear. Using golden Syrian hamsters infected with an early circulating SARS-CoV-2 strain harboring the D614G mutation in the spike protein; we show here that rather than being related to a first wave of apoptosis as proposed in previous studies, the innate immune cells play a major role in the destruction of the olfactory epithelium. We observed that while apoptosis remains at a low level in the damaged area of the infected epithelium, the latter is invaded by Iba1$^+$ cells, neutrophils and macrophages. By depleting the neutrophil population or blocking the activity of neutrophil elastase-like proteinases, we could reduce the damage induced by the SARS-CoV-2 infection. Surprisingly, the impairment of neutrophil activity led to a decrease in SARS-CoV-2 infection levels in the olfactory epithelium. Our results indicate a counterproductive role of neutrophils leading to the release of infected cells in the lumen of the nasal cavity and thereby enhanced spreading of the virus in the early phase of the SARS-CoV-2 infection.

Keywords Post-viral olfactory disorder (PVOD) · Pathophysiology · Innate immunity

Abbreviations

OE	Olfactory epithelium
OSN	Olfactory sensory neuron
MPO	Myeloperoxidase

Introduction

Loss of smell (anosmia) is a major symptom of COVID-19 pandemic. With omicron's increased transmission, hundreds of thousands of people per day still get infected worldwide. Despite omicron's reduced anosmia prevalence [1], loss of smell will likely affect millions more [2, 3] and 10% of anosmic patients might not recover their sense of smell 6 months after the disease onset [4, 5]. The full olfactory recovery could even take up to 1 year and some patients may never recover their sense of smell [6]. A recent study estimates that in the USA about 720,000 people actually suffer from chronic olfactory disorder related to COVID-19 [7]. The loss of smell negatively impacts life quality by disrupting feeding behavior potentially leading to malnutrition; and by exposing to food poisoning and to inhalation of dangerous chemicals [8]. In severe and persistent cases, anosmic patients could possibly suffer from chronic depression [9]. It is thus crucial to understand the cellular basis of anosmia.

Olfaction starts in the olfactory epithelium (OE) which contains olfactory sensory neurons (OSNs) surrounded by supporting cells called sustentacular cells. Both cell types are regenerated regularly due to multipotent basal cells [10]. Among these cells, only sustentacular cells express significantly angiotensin-converting enzyme 2 (ACE2) and transmembrane serine protease 2 (TMPRSS2) required for

✉ Nicolas Meunier
nicolas.meunier@inrae.fr

1 Unité de Virologie et Immunologie Moléculaires (UR892), INRAE, Université Paris-Saclay, Jouy-en-Josas, France

2 INSERM UMR-1100, "Research Center for Respiratory Diseases" and University of Tours, 37032 Tours, France

3 UMR 1161 Virologie, INRAE-ENVA-ANSES, École Nationale Vétérinaire d'Alfort, Maisons-Alfort, 94704 Paris, France

SARS-CoV-2 cellular entrance [11–13]. We and others observed in the golden Syrian hamster model that SARS-CoV-2 infects massively the sustentacular cells in the OE leading to its desquamation as well as olfactory neurons deciliation and death [14–16]. Although very rarely OSNs may be infected by SARS-CoV-2 [17], a recent study in humans confirms that anosmia arises primarily from infection of sustentacular cells of the OE followed by the disruption of OE integrity without OSN infection [18].

In this study, we focused on the early events following SARS-CoV-2 infection of the nasal cavity to explore the mechanism of the unusually extensive OE damage following SARS-CoV-2 infection. Several studies reported that most cells of the infected OE including OSNs undergo apoptosis [19–22]. A similar phenomenon has been reported during influenza infection [23] and has been considered for SARS-CoV-2 as a defense mechanism to limit a potential invasion of the central nervous system by pathogens using the olfactory route [24]. Alternatively, innate immune cells could trigger directly the desquamation of the OE through inflammation as observed in the lung [25]. Indeed, innate immune cells invade massively the SARS-CoV-2-infected OE [14]. Iba1 (ionized calcium-binding adapter molecule 1) is a marker of microglia/macrophages [26] which are the most studied innate immune cells in the nasal cavity [23]. In the central nervous system, Iba1$^+$ microglial cells ensure viral clearance by phagocytizing viral particles and infected cells [27, 28] and can induce cell death as observed in the hippocampus using the Theiler's virus model of encephalitis [29]. As the OE is not protected by the blood–brain barrier, neutrophils and monocytes/macrophages classically recruited during the early event of inflammation could also be involved in the OE damage following SARS-CoV-2 infection [30, 31]. Neutrophils are well known for their ability to induce tissue damage, notably through the release of elastase-like proteinases [32, 33] as well as the production of reactive oxygen species (ROS) by the myeloperoxidase (MPO) and formation of toxic neutrophil extracellular traps [34, 35]. Macrophages are known for their ability to phagocyte pathogens, produce cytokines and activate other immune cells [36]. Although they are involved in the regeneration of the OE [37, 38], they can also lead to tissue damage during viral infections notably through NLRP3 (NOD-, LRR- and pyrin domain-containing protein 3) inflammasome activation and metalloproteinases activity [31].

In the current work, we observed that apoptosis remains at a low level in the infected areas of the OE while innate immune cells were systematically present in the damaged area of the OE. By manipulating neutrophil activity by two different complementary approaches, we show that they play a major role in the early events of OE destabilization following SARS-CoV-2 infection.

Material and methods

Study design

The study was performed to understand the cellular mechanisms leading to the SARS-CoV-2-induced damage in the OE using hamsters as an animal model. Hamsters experiments were planned in accordance with the principles of the 3Rs (replacement, reduction and refinement). Body weight and animal behavior were monitored before and during the experiments. Different parameters in the nasal cavity were measured by quantitative polymerase chain reaction (qPCR) and by immunohistochemistry. SARS-CoV-2 replication was measured in vitro to evaluate a potential inhibition by the drugs used to modulate neutrophils activity. Sample size for each experiment is indicated in figure legends. During analysis, all data points were included except because of technical failure to process the sample. Animals were randomized to the experimental groups. All analyses were performed blindly of the treatment.

SARS-CoV-2 isolates

In vivo experiments were carried out with SARS-CoV-2 strain BetaCoV/France/IDF/200107/2020, which was isolated by Dr. Paccoud from the La Pitié-Salpétrière Hospital in France. This strain was kindly provided by the Urgent Response to Biological Threats (CIBU) hosted by Institut Pasteur (Paris, France), headed by Dr. Jean-Claude Manuguerra. Cell culture experiments were performed with the SARS-CoV-2 strain France/IDF0372/2020 kindly provided by Sylvie van der Werf. Both strains have been isolated in the beginning of the pandemic in Europe in March 2020.

Animals

Fifty-six 8-week-old male hamsters were purchased from Janvier's breeding Center (Le Genest, St Isle, France). Animal experiments were carried out in the animal biosafety level 3 facility of the UMR Virologie (ENVA, Maisons-Alfort); approved by the ANSES/EnvA/UPEC Ethics Committee (CE2A16) and authorized by the French ministry of Research under the number APAFIS#25384-2020041515287655.

Infection was achieved by nasal instillation (40 µL in each nostril with 5.10^3 $TCID_{50}$ of SARS-CoV2 strain BetaCoV/France/IDF/200107/2020) on anesthetized animals under isoflurane. Such viral infection dose gives robust infection level in the nasal cavity [14, 39]. Seven mock-infected animals received only Dulbecco's minimal essential medium.

For neutrophil depletion experiments, hamsters were injected intraperitoneally with either PBS or 150 mg/kg

and 100 mg/kg of cyclophosphamide (CAS: 6055-19-2; PHR1404; Sigma-Aldrich), respectively, at 3 and 1 days before SARS-CoV-2 infection. Animals were sacrificed at 1 dpi (days post-infection) and at 2 dpi ($n=4$ in each group).

To inhibit neutrophil elastase-like proteases, we used a specific synthetic cathepsin C inhibitor ($IcatC_{XPZ-01}$; [40] diluted in 10% (2-Hydroxypropyl)-β-cyclodextrin (CAS: 128446-35-5; C0926; Sigma-Aldrich) suspended in citrate buffer 50 mM at pH 5 (vehicle) as described previously [41]. Hamsters were injected intraperitoneally twice a day with either vehicle ($n=4$) or $IcatC_{XPZ-01}$ at 4.5 mg/kg for 10 days before infection by SARS-CoV-2 ($n=4$). Animals were sacrificed at 1 dpi.

For all experiments except $IcatC_{XPZ-01}$ treatment, the head was divided sagittally into two halves, of which one was used for immunohistochemistry experiments. Nasal turbinates were extracted from the other half for qPCR analysis. Only histological analysis was performed on tissues from $IcatC_{XPZ-01}$ treatment experiments.

Histology, immunohistochemistry and quantifications

The immunohistochemistry analysis of the olfactory mucosa tissue sections was performed as described previously in mice [43]. Briefly, the animal hemi-heads were fixed for 3 days at room temperature in 4% paraformaldehyde (PFA) and decalcified in Osteosoft (101728; Merck Millipore; Saint-Quentin Fallavier; France) for 3 weeks. Blocks were cryo-protected in 30% sucrose. Cryo-sectioning (12 µm) was performed in coronal sections of the nasal cavity, perpendicular to the hard palate in order to examine the vomeronasal organ (VNO), olfactory epithelium (OE), Steno's gland and olfactory bulb. Sections were stored at − 80 °C until use.

Non-specific staining was blocked by incubation with 2% bovine serum albumin (BSA) and 0.05% Tween. The sections were then incubated overnight with primary antibodies directed against SARS nucleocapsid protein (1/500; mouse monoclonal; clone 1C7C7; Sigma-Aldrich), ionized calcium-binding adapter molecule 1 (Iba1) (1/500; rabbit monoclonal; clone EPR16588; Abcam), myeloperoxidase protein (MPO) (1/500; rabbit monoclonal; clone EPR20257; Abcam), CD68 (1/200; rabbit polyclonal; PA1518; Boster), cleaved caspase 3 (C3C) (1/200; rabbit polyclonal; #9661; Cell signaling), G_{olf} (1/300; rabbit polyclonal; C-18; Santa Cruz), Olfactory Marker Protein (OMP) (1/500; goat polyclonal; 544-10001; Wako) and CK18 (1:50; mouse polyclonal; MAB3234—RGE53, Sigma-Aldrich). Fluorescence staining was performed using goat anti-mouse-A555; goat anti-rabbit-A488 and donkey anti-goat-A546 (1/800; Molecular Probes A21422; A11056; A11008, respectively; Invitrogen).

Images were taken using a 1X71 Olympus microscope equipped with an Orca ER Hamamatsu cooled CCD camera (Hamamatsu Photonics France; Massy; France) or with a Zeiss LSM 700 confocal 187 microscope for cleaved caspase 3 co-staining with either OMP or CK18 experiment and MPO co-staining with Hoechst stained multi-lobal nuclei (MIMA2 Platform, INRAe). Whole section images were reconstructed from 3 images taken at × 50 magnification using a Leica MZ10F Fluorescent binocular microscope. We used these images to display the level of infection revealed by TRITC fluorescence. As this binocular did not possess any UV filter to display Hoechst fluorescence, we used the FITC channel green autofluorescence to display the turbinates structures.

To assess olfactory epithelium damage, we scored the integrity of the OE from 1 to 9 based on Hoechst staining according to missing nuclei area, irregularity of the OE structure and increased distance between nuclei indicating loosening of the epithelium leading to desquamation (Supp. Fig. 1). To evaluate the correlation of apoptosis and innate immune cell presence with damage, OE areas were divided in two groups: undamaged areas (damage score equal to 1 or 2) and damaged areas (damage score between 5 and 9). Apoptosis level, infiltration of immune cells in the OE and its underlying lamina propria were quantified as the percentage of the area positive for C3C (cleaved caspase 3); Iba1 (macrophages/microglia), CD68 (activated bone-marrow-derived macrophages) and MPO (neutrophils). For each animal, the percentage of stained OE was averaged over 4 distinct areas in the beginning of olfactory turbinates at 1 dpi and in the medial part of the nasal cavity containing Steno's gland and NALT at 2 dpi.

In cyclophosphamide and in $IcatC_{XPZ-01}$ experiments, we performed both IHC and classical hematoxylin and eosin (HE) staining as described previously [42]. We examined two independent sections of nasal turbinates (separated by 500 µm) in the middle of the nasal cavity containing NALT and Steno's gland. For each section, we measured the total infected area of the OE, the area of desquamated cells in the lumen (based on Hoechst nuclear staining) and the percentage of infected desquamated cells in the lumen (based on N protein immunostaining). These experiments were designed to measure the global damage of the OE following SARS-CoV-2 infection when neutrophil action was impaired. At 2 dpi, the level of neutrophil infiltration was so high that complete quantification could not be achieved. Instead, we set a global score from 1 to 9 of $^{1}/$OE damage based on the integrity of the OE and $^{2}/$neutrophil infiltration based on the overall presence of MPO signal in nasal mucosa and in nasal cavity lumen. We verified that our scoring system and total quantification gave similar results for MPO^{+} cells presence at 1 dpi where infection is restricted to the most ventro rostral part of the nasal turbinates.

All quantifications were made with ImageJ (Rasband, W.S., ImageJ, US National Institutes of Health, Bethesda, Maryland, USA, http://imagej.nih.gov/ij/, 1997–2012) to threshold specific staining and performed blindly of the treatment.

RNA extraction and RT-qPCR analysis

Total RNA was extracted from frozen nasal turbinates using the Trizol-chloroforme method as described previously [43]. Oligo-dT first strand cDNA synthesis was performed from 5 µg total RNA with iScript Advance cDNA Synthesis Kit for RT-qPCR (BioRad; #1725038) following manufacturer's recommendations. qPCR was carried out using 125 ng of cDNA added to a 15 µL reaction mix. This reaction mix contained 10 µL iTaq Universal Sybr Green SuperMix (Bio-Rad; #1725124), and primers at 500 nM (sequences in Supp Table 1). The reaction was performed with a thermocycler (Mastercycler ep Realplex, Eppendorf). Fluorescence during qPCR reaction was monitored and measured by Realplex Eppendorf software. A dissociation curve was plotted at the end of the forty amplification cycles of the qPCR to check the ability of theses primers to amplify a single and specific PCR product.

Quantification of initial specific RNA concentration was done using the ΔΔCt method. Standard controls of specificity and efficiency of the qPCR were performed. The mRNA expression of each gene was normalized with the expression level of G3PDH. A correction factor was applied to each primer pair according to their efficiency [44].

Measure of antiviral activity of cyclophosphamide and cathepsin C inhibitor against SARS-CoV-2 in cell culture

Vero E6 cells (CRL-1586, ATCC maintained at 37 °C; 5% CO_2) were seeded at 2.10^4 cells per well in a 96-well plate in Dulbecco's Modified Eagle's Medium, 5% fetal bovine serum (FBS-12A, Capricorn Scientific, Clinisciences). For cyclophosphamide antiviral activity evaluation, cells were treated with 0.15 mg/mL (corresponding to the maximum dose potentially present in hamsters) or 0.45 mg/mL cyclophosphamide diluted in sterile PBS. For $IcatC_{XPZ\text{-}01}$ antiviral activity evaluation, cells were treated with 4.5 µg/mL (corresponding to the maximum dose potentially present in hamsters) or 13.5 µg/mL $IcatC_{XPZ\text{-}01}$ diluted in 10% dextrin, citrate buffer 50 mM, pH = 5. Cells were treated with PBS as control ($n = 6$ for each condition) and molecule cytotoxicity was tested as well without infection at the highest used concentration. All treatments were started one hour prior to infection with SARS-CoV-2 strain France/IDF0372/2020 at 5×10^3 pfu per well diluted in DMEM, 10% fetal bovine serum. Loss of cell viability reflecting the efficiency of viral infection was measured 3 days after infection by adding 100 µL Cell Titer-Glo reagent to each well (CellTiterGlo Luminescent Cell Viability Assay, Promega #G7571), according to the manufacturer's protocol. Cell luminescence of each well was then quantified using an Infinite M200Pro TECAN and normalized to the control condition.

Statistical analysis

All comparisons were made using Prism 5.0 (GraphPad). Statistical significance between groups was assessed using nonparametric Mann–Whitney tests. For correlation analyses, we used Spearman nonparametric test. Error bars indicate the SEM. Detailed information on statistical test used, sample size and P value are provided in the figure legends.

Results

Apoptosis occurs after cell desquamation following SARS-CoV-2 infection of the olfactory epithelium

We previously observed that as soon as two days following nasal instillation of SARS-CoV-2 in Syrian gold hamsters, the sustentacular cells of the OE were massively infected along with strong cellular loss and cellular debris filling the lumen of the nasal cavity [14]. In order to understand the events leading to this desquamation, we chose to focus on the early stages of infection at 1 and 2 dpi. To evaluate the importance of apoptosis in the damage of the OE following SARS-CoV-2 infection, we measured the level of cleaved caspase 3 signal in uninfected animals, and in infected zones of the OE that were either intact or damaged (Fig. 1). Basal level of apoptosis occurring in the OE was not increased in either zone at 1 or 2 dpi (Fig. 1D). However, we observed a strong cleaved caspase 3 signal co-localizing partly with desquamated cell in the lumen of the nasal cavity. The cleaved caspase 3 signal in the lumen of the nasal cavity was increased 5- and 14-fold compared to the OE at 1 and 2 dpi, respectively, which was statistically significant at 2 dpi (Mann–Whitney, $p = 0.0286$) and nearly significant at 1 dpi ($p = 0.0525$). In order to examine the potential OE origin of the C3C positive cells, we performed double staining with cleaved caspase 3 and CK18 or OMP (specific markers of sustentacular cells and OSN, respectively). We observed that most apoptotic cells co-stained with OMP but not with CK18, indicating that OSN but not sustentacular cells undergo Caspase 3 apoptosis once released in the lumen of the nasal cavity (Supp. Fig. 2).

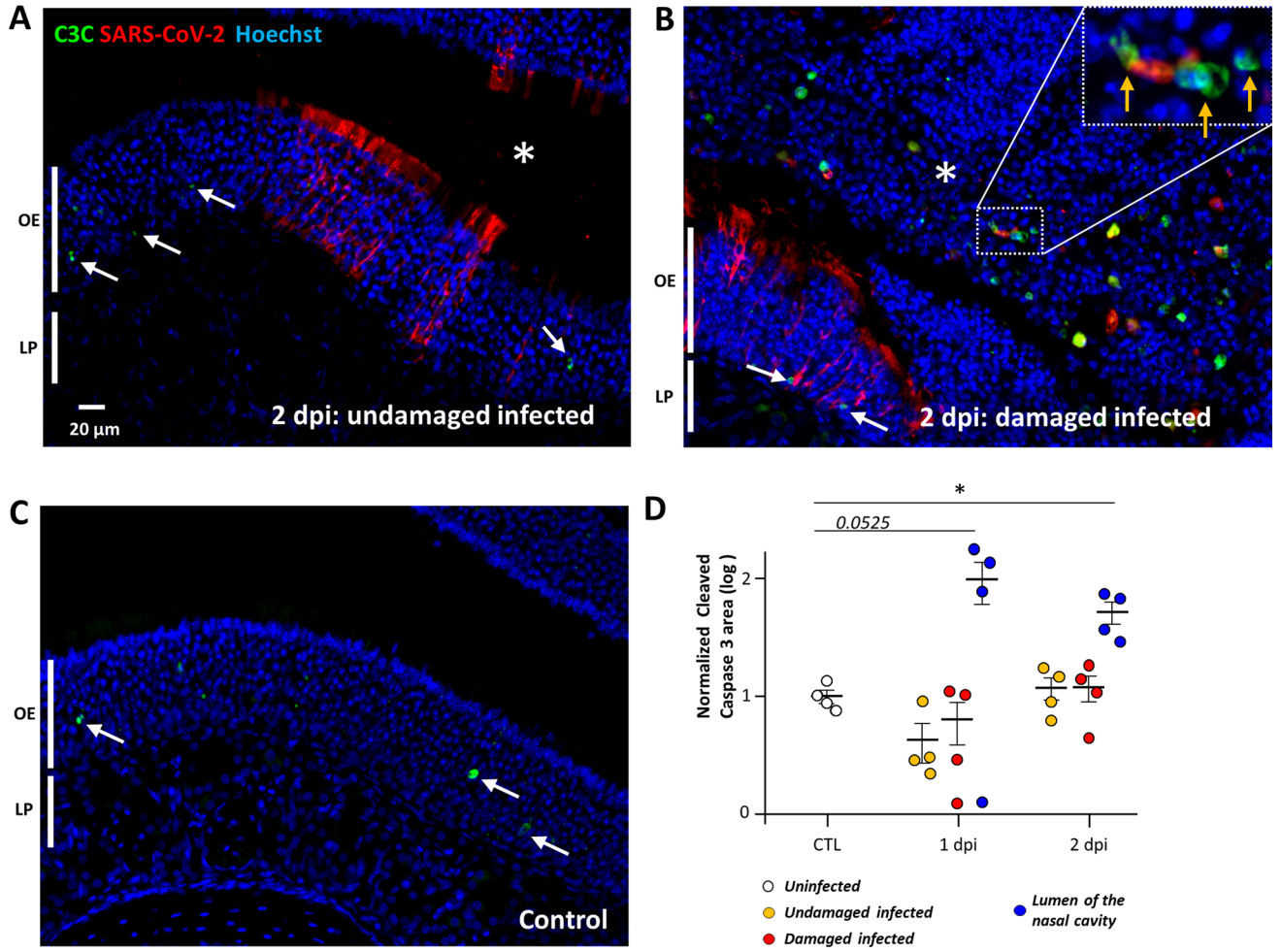

Fig. 1 Apoptosis occurs in desquamated cells in the lumen of the nasal cavity following SARS-CoV-2 infection but not in the olfactory epithelium. Representative images of an infected intact (**A**), infected damaged (**B**) area of the olfactory epithelium at 2 days post-infection (dpi) and in a control animal (**C**). Apoptotic cells in the olfactory epithelium are indicated by a white arrow (OE; olfactory epithelium/LP lamina propria). The lumen of the nasal cavity is indicated by a white asterisk and is filled with cells, some of which colocalize in their nucleus cleaved caspase 3 signal (orange arrow). (**D**) Cleaved caspase 3 signal in the olfactory epithelium normalized to control (log 10, Mean ± SEM, $n = 4$, $^*p < 0.01$ (Mann–Whitney test))

Damage of the infected olfactory epithelium is correlated with infiltration of innate immune cells

Since apoptosis does not significantly occur in the OE during the initial phase of infection, the desquamation of the infected OE may be related to immune cell infiltration [14, 15]. So far, the immune cells in the nasal cavity have been poorly characterized. Neutrophils and macrophages are known for their importance in clearing infected tissue [45], but only Iba1$^+$ cells presence is well characterized in the OE [23]. Iba1$^+$ cells are described as microglia/macrophages, but CD68 is more classically used as a marker of monocytes and macrophages [46]. Concerning neutrophils, the presence of neutrophil cytosol factor 2 (Ncf2; [47]) and myeloperoxidase (MPO) have been used successfully to characterize these cells in hamsters [48]. As MPO is only expressed during neutrophil maturation in the bone marrow [49], we used Ncf2 as a marker of neutrophil presence by qPCR and MPO by immunohistochemistry.

We first evaluated at 1 dpi and 2 dpi by qPCR the expression of Iba1, CD68 and Ncf2 along with classical inflammatory markers (TNFα and IL6) and the presence of the virus (Supp. Fig. 3). At 1 dpi, SARS Nucleocapsid protein (SARS N) was already abundantly expressed in the OE at a similar level as at 2 dpi, and TNFα and IL6 transcripts increased gradually (Mann–Whitney, $p < 0.05$). Iba1 and CD68 expression related to macrophage presence in the OE did not rise significantly at 1 dpi compared to control (Mann–Whitney, $p = 0.164$ and 0.128, respectively) but did at 2 dpi (Mann–Whitney, $p < 0.05$). Concerning neutrophils, Ncf2 expression was strongly enhanced at 1 dpi and was still increasing at 2 dpi (Mann–Whitney, $p < 0.05$). These

results suggest that neutrophils are already recruited at 1 dpi and that their recruitment continues at 2 dpi along with the arrival of Iba1$^+$ and CD68$^+$ cells.

We next focused on immunostaining to characterize the presence of Iba1$^+$, CD68$^+$ and MPO$^+$ cells. In the OE of an uninfected hamster, Iba1$^+$ cells were already present and mainly localized in the lamina propria while CD68 signal was absent (Fig. 2A), indicating that Iba1$^+$ cells do not express the classical CD68 marker of macrophages. This was confirmed in the infected areas of the OE where we observed a very different presence of Iba1$^+$ and CD68$^+$ cells. Iba1$^+$ cells were massively present as soon as 1 dpi in the damaged parts of the infected OE as well as in the desquamated cells in the lumen of the nasal cavity. CD68$^+$ cells were less abundant in the damaged part of the OE and mainly present in the desquamated cells filling the lumen of

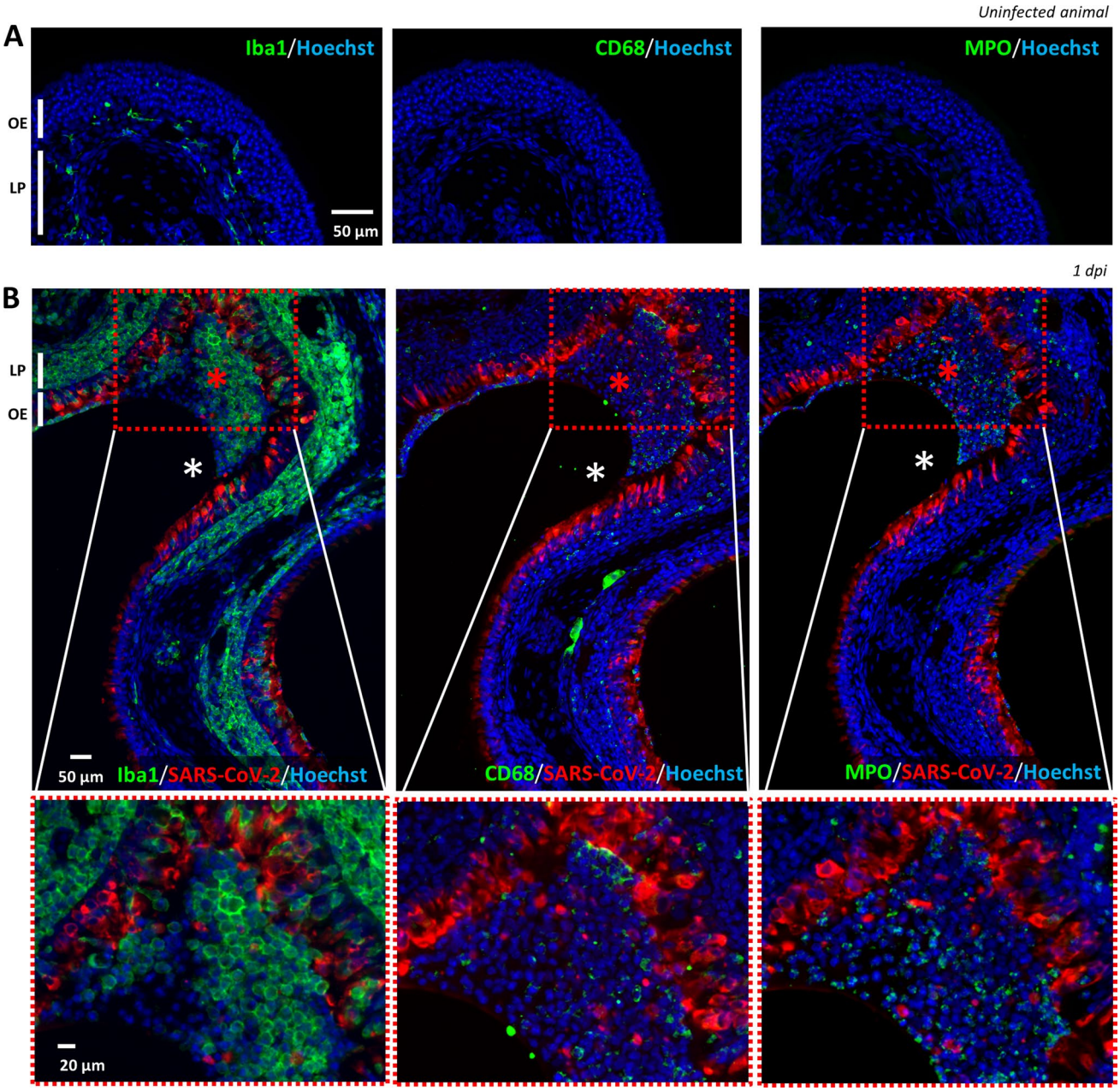

Fig. 2 Iba1$^+$ (microglia/monocyte lineage), CD68$^+$ (macrophages) and MPO$^+$ (neutrophils) cells presence in the olfactory epithelium before and during SARS-CoV-2 infection. Immunostaining on successive slides of the olfactory epithelium from a non-infected (**A**) or 1 dpi hamster (**B**). Only Iba1$^+$ cells are present in the uninfected olfactory epithelium (OE) and in the lamina propria (LP). In the infected epithelium, Iba1$^+$ cells are massively present in the OE while CD68$^+$ and MPO cells are mostly present in the desquamated cells (red asterisk) in the lumen of the nasal cavity (white asterisk)

the nasal cavity (Fig. 2B). A double staining against Iba1 and CD68 of the desquamated cells in the lumen of the nasal cavity did not reveal any overlap of the two markers (Supp. Fig. 4), showing that Iba1$^+$ cells do not express CD68 once they are located among the desquamated cells. Similar to CD68, MPO signal was absent in uninfected OE and appears during infection partly in the damaged OE and mainly in the lumen of the nasal cavity along with desquamated cells. The MPO$^+$ cells possess typical multi-lobal nuclei characteristic of neutrophils (Supp. Fig. 5). Overall, these results show that Iba1$^+$ cells are much more abundant in the infected OE than CD68$^+$ macrophages and MPO$^+$ neutrophils cells, both being mainly present in the desquamated cells filling the lumen of the SARS-CoV-2-infected nasal cavity.

If these innate immunity cells are involved in the desquamation of the OE, we should always observe their presence in the damaged infected area of the OE. To investigate their infiltration in the OE and its correlation with damage, we focused on three zones similarly as for apoptosis quantification: $^{1/}$uninfected, infected $^{2/}$without or $^{3/}$with damage at 1 and 2 dpi. The infiltration level of Iba1$^+$ cells in the OE was increased in the damaged infected zone but not in the undamaged one (Fig. 3). This difference was statistically significant at 2 dpi (Mann–Whitney, $p=0.0286$) and nearly significant at 1 dpi ($p=0.0525$). The infiltration of these cells was similarly increased in the lamina propria underneath the previous OE zones with a significant difference at 2 dpi ($p=0.0286$). We observed a significant correlation between the damage of the OE and their presence in both the OE and the underlying lamina propria (Spearman test, $p=0.0098$ and 0.0006, respectively).

We similarly examined whether the presence of CD68$^+$ macrophages and MPO$^+$ neutrophils in the OE was associated with the damage of the OE after SARS-CoV-2 infection. Both CD68 and MPO signals were increased in the damaged infected zone but not in the undamaged one (Fig. 4). This difference was statistically significant in the infected damaged zones at 1 and 2 dpi for both markers compared to control and infected undamaged zones of the OE and lamina propria (Mann–Whitney, $p<0.05$). We observed a significant correlation between the damage of the OE and the presence of both CD68$^+$ and MPO$^+$ cells in the OE and the lamina propria (Spearman test, $p<0.001$).

Neutropenia reduces damage of the OE related to SARS-CoV-2 infection as well as OE infected area

Neutrophils are the main actors of damage to the olfactory epithelium during Poly(I:C)-induced inflammation [50]. We therefore evaluated whether a neutropenic treatment based on cyclophosphamide would reduce the damage induced by SARS-CoV-2 infection in the OE. Such treatment causes apoptosis of bone-marrow-derived cells and has previously been used successfully on hamsters to induce neutropenia [48]. We first monitored in control animals how the treatment impacts circulating immune cells. Neutrophils population was decreased by ~ tenfold, lymphocytes were also decreased by ~ threefold, and monocytes by ~ fivefold (Supp. Fig. 6A). Since cyclophosphamide can impact basal cell proliferation and thus OE structure, we examined its effect in uninfected animals and did not observe any evident damage on the OE structure (Supp Fig. 6B). We next examined the impact of this treatment on the expression of genes related to the innate immune system in the nasal turbinates during SARS-CoV-2 infection. At 1 dpi, the expression of Iba1 and CD68 was not statistically different between vehicle and cyclophosphamide treated animals but a decrease of Ncf2 expression reflecting a reduced presence of neutrophils almost reached significance (Mann–Whitney; $p=0.0571$; Fig. 5A). We observed a tendency of TNFα and IL6 expression reduction which did not reach significance either ($p=0.1143$). Despite the overall tendency of a decrease of innate immune system response at 1 dpi, the level of SARS-CoV-2 infection reflected by N protein expression was decreased and the difference almost reached significance ($p=0.0571$). At 2 dpi, the expression of all genes related to innate immune cell presence as well as TNFα was decreased ($p<0.05$). We examined histologically the neutrophil presence, damage, level of infection in the OE (Fig. 5B, C and Supp. Figs. 6C, 7). MPO signal was significantly decreased at 1 dpi in the OE of cyclophosphamide treated animals compared to control ($p<0.05$) (Fig. 5D$_1$). The damage in the OE was significantly decreased at 1 and 2 dpi ($p<0.01$ and $p<0.05$, respectively) (Fig. 5D$_2$ and Supp. Figs. 8, 9). The reduction tendency of the virus presence measured by the N protein expression was confirmed by immunostaining in the OE at 1 dpi only ($p<0.05$; Fig. 5D$_3$) and seems specific to the OE as the infection of the Steno's gland epithelium lining the maxillary sinus was similar in both conditions (Supp. Fig. 8). We hypothesize that this reduction could be linked to less infected desquamated cells released into the lumen of the nasal cavity following the OE damage induced by the neutrophils. We thus quantified the area of desquamated cells in the lumen which was significantly decreased at 1 dpi and almost reached significance at 2 dpi (Fig. 5D$_4$; $p<0.001$ and $p=0.0905$, respectively). In the desquamated cells of the lumen, the percentage of infected cells was significantly diminished at 1 dpi (Fig. 5D$_5$; $p<0.001$) but not at 2 dpi when infected desquamated cells were in the lumen of the nasal cavity in some treated animals (Supp Fig. 6C). Since the reduction of OE infected area of immunocompromised animal was unexpected, we verified that a dose three times higher than the maximum dose of cyclophosphamide potentially present in the hamsters during infection did not limit the virus replication in vitro (Supp. Fig. 10A, C).

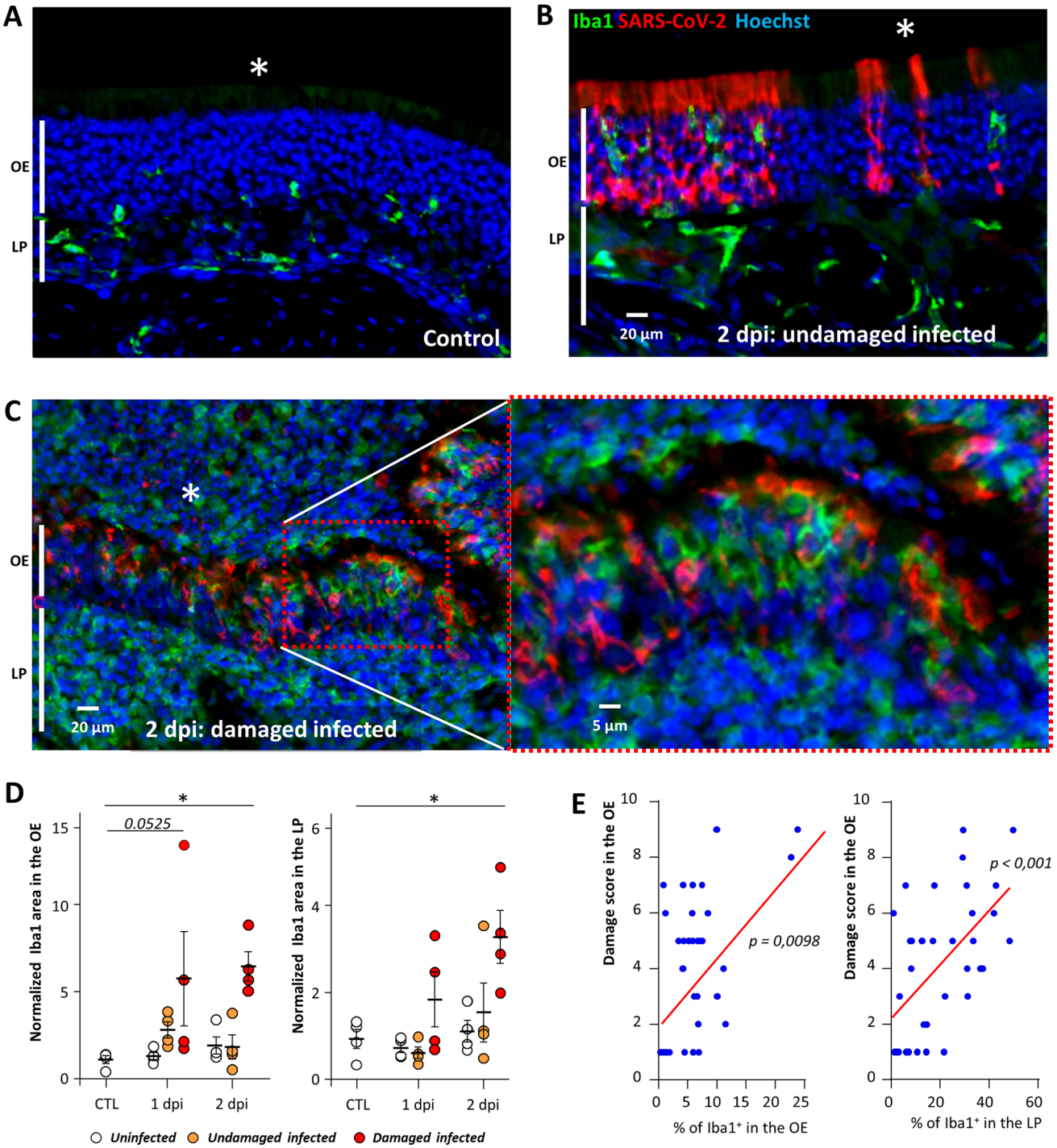

Fig. 3 Iba1$^+$ cell infiltration increases with the damage in the OE. Representative images of the olfactory epithelium from an uninfected animal (**A**), infected but undamaged (**B**) and infected and damaged (**C**) area of the olfactory epithelium (OE) at 2 days post-infection (dpi). The lumen of the nasal cavity is indicated by a white asterisk. (**D**) Iba1$^+$ signal in the olfactory epithelium (OE, left) and lamina propria (LP, right) in control animals (CTL) or at 1 or 2 dpi (Mean normalized to control ± SEM, $n = 4$, $^*p < 0.01$ (Mann–Whitney test)). (**E**) Correlation between score damage of the olfactory epithelium and the percentage of Iba1$^+$ signal in the olfactory epithelium (left panel) and the lamina propria (right panel). Spearman test p value

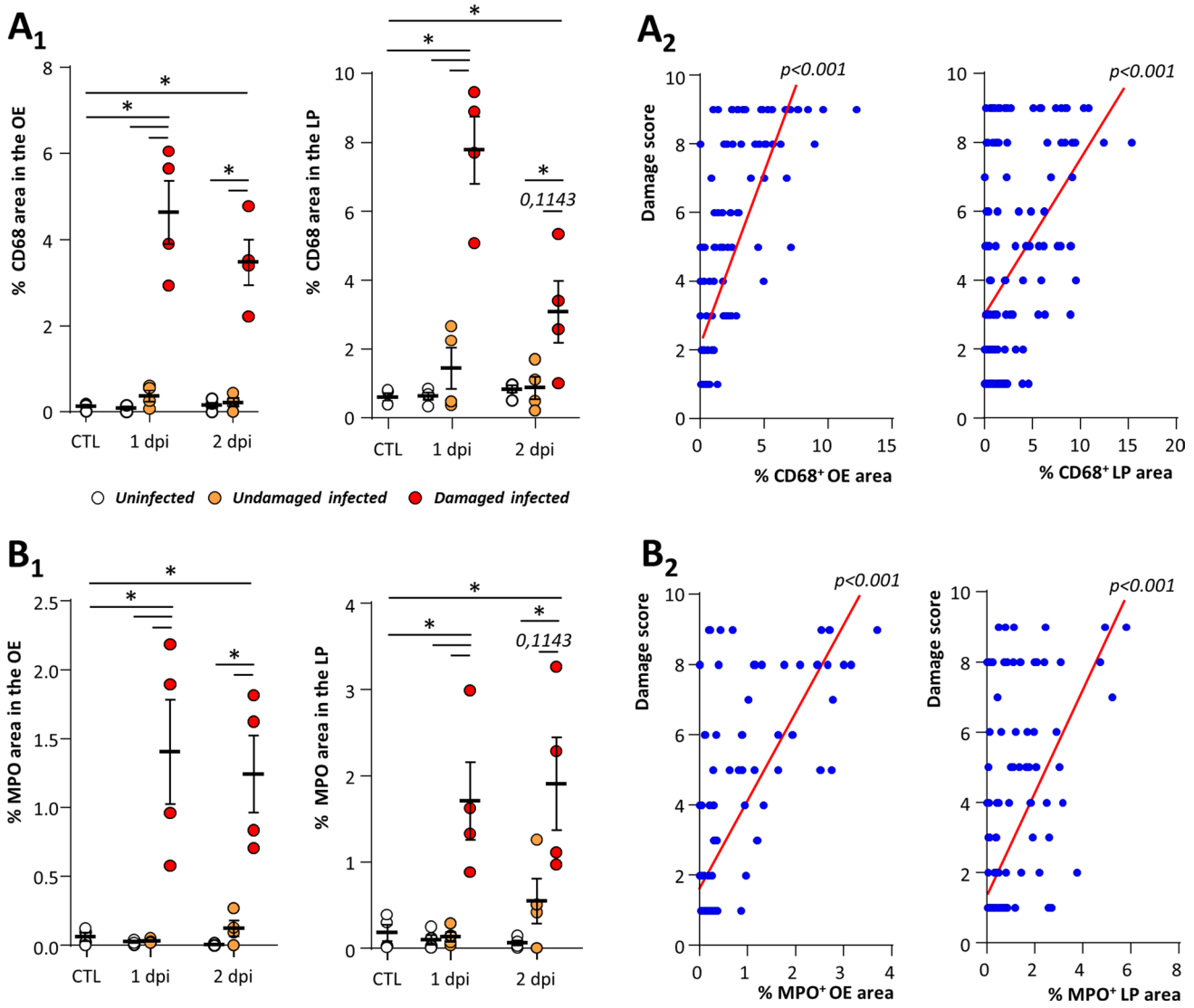

Fig. 4 $CD68^+$ macrophage and MPO^+ neutrophil cells are associated with damage of the olfactory epithelium during SARS-CoV-2 infection. $CD68^+$ ($\mathbf{A_1}$) and MPO^+ ($\mathbf{B_2}$) signal in the olfactory epithelium (OE, left) and lamina propria (LP, right) in either control animals (CTL) or at 1 or 2 days post-infection (dpi) (Mean normalized to control ± SEM, $n = 4$, $^*p < 0.05$ (Mann–Whitney test)). Correlation between score damage and percentage of $CD68^+$ ($\mathbf{A_1}$) and MPO^+ ($\mathbf{B_2}$) signal in the olfactory epithelium (left panel) and the lamina propria (right panel). Spearman test p value

Inhibition of neutrophil proteinases reduces damage of the OE related to SARS-CoV-2 infection as well as infected OE area

In order to confirm our results on cyclophosphamide treatment which affects immune cells other than neutrophils, we treated animals with an inhibitor of cathepsin C ($IcatC_{XPZ\text{-}01}$) which is essential for the maturation of elastase-like proteinases of neutrophils. This inhibitor has been used successfully to almost completely eliminate the elastase-like activity of neutrophils in vivo [41]. We chose to focus on the histological impact of $IcatC_{XPZ\text{-}01}$ treatment at 1 dpi as it gave the most significant results during cyclophosphamide treatment.

The inhibition of elastase-like proteinases of neutrophils gave similar results as cyclophosphamide with the exception of some limited neutrophil infiltration in the infected OE (Fig. 6A, B). Globally, the MPO^+ neutrophil presence in the nasal turbinates and the damage in the infected area of the OE were significantly reduced compared to vehicle treated animals (Fig. $6C_1$ and Supp. Figs. 11 and 12; Mann–Whitney; $p < 0.01$). We also observed significantly less desquamated cells in the lumen of the nasal cavity which were also less infected (Fig. $6C_2$; Mann–Whitney; $p < 0.01$). Since we observed again that the inhibition of neutrophil action limited SARS-CoV-2 presence in the OE, we verified that a dose three times higher than the maximum

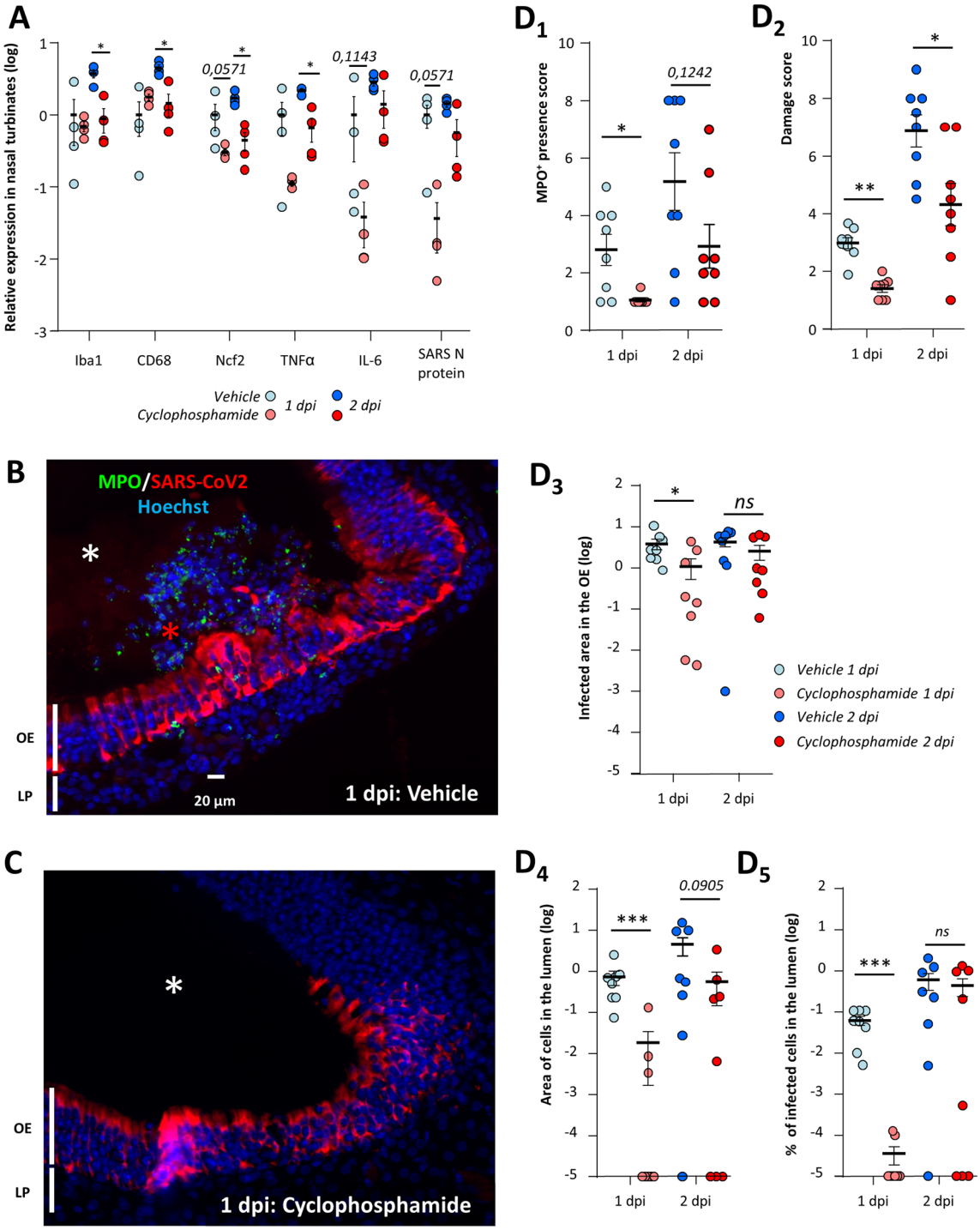

dose of $IcatC_{XPZ\text{-}01}$ potentially present in the hamsters during infection did not impair the virus replication in vitro (Supp. Fig. 10B, C). We also observed that the reduction of SARS-CoV-2 infection by $IcatC_{XPZ\text{-}01}$ was specific to the OE as the infection of Steno's gland epithelium was not affected in presence of cathepsin C inhibitor (Supp. Fig. 11).

Discussion

The anosmia induced by SARS-CoV-2 infection is now clearly linked to the infection of the olfactory epithelium with a main tropism for sustentacular cells [18, 51]. We and others have observed that following this infection, the OE undergoes massive damage leading to cell desquamation and

◂**Fig. 5** Immunosuppression induced by cyclophosphamide reduces damage of the olfactory epithelium as well as OE infection area. (**A**) Expression of innate immune genes in the nasal turbinates with or without cyclophosphamide treatment at 1 and 2 days post-infection (dpi). Iba1, CD68 and Ncf2 are related to the presence of microglia/macrophages, monocytes/macrophages and neutrophils, respectively; TNFα and IL6 are two cytokines expressed during inflammation; SARS-CoV-2 N expression is related to the SARS-CoV-2 infection. Results represent the Mean ± SEM relative to vehicle-treated hamsters ($n=4$, $*p<0.05$; Mann–Whitney test). Representative images of the infected olfactory epithelium immunostained for MPO (neutrophil marker) and SARS-CoV-2 N protein in (**B**) vehicle and (**C**) cyclophosphamide treated animal (olfactory epithelium (OE), lamina propria (LP)). In the vehicle condition, the lumen (white asterisk) is filled with desquamated cells (red asterisk) containing MPO signal. In the cyclophosphamide condition, MPO signal is absent and the lumen is mostly free of cellular debris**.** Quantification in the OE of ($\mathbf{D_1}$) MPO^+ neutrophil presence ($\mathbf{D_2}$) damage score ($\mathbf{D_3}$) SARS-CoV-2-infected area and in the lumen of the nasal cavity of ($\mathbf{D_4}$) desquamated cells area and ($\mathbf{D_5}$) percentage of SARS-CoV-2-infected area in the desquamated cells (Mean ± SEM, $n=8$ areas of the nasal cavity from 4 different animals, $*p<0.05$, $**p<0.01$, $***p<0.001$ (Mann–Whitney))

cellular debris filling the lumen of the nasal cavity [14, 21, 22], but the mechanism of this destruction is less clear.

Several studies reported an increase in apoptosis especially in olfactory sensory neurons [20–22] and assumed that it led to the destruction of the OE. Here, we first examined the apoptosis level based on cleaved caspase 3 level in the OE of uninfected animals and infected areas of the OE, either intact or damaged. If apoptosis initiates the desquamation process then it should increase in the damaged areas of the OE. However, we observed a similar level of apoptosis level in all these areas (Fig. 1D), which was consistent with the basal level of apoptosis that we previously measured in adult mice and rats OE [42, 52]. While the apoptosis in the infected damaged OE was low, we observed an increased level of apoptosis in cells present in the lumen of the nasal cavity. The discrepancy with previous studies may be due to different models as some were performed using transgenic mice expressing hACE2, but it should be noted that these studies did not perform any quantification and observed as well apoptosis staining in the lumen of the nasal cavity [22]. We observed that most apoptotic cells co-stained with OMP specifically expressed by mature OSNs but not CK18 specific of sustentacular cells (Supp Fig. 2B), indicating that the OSNs undergo C3C-linked apoptosis once released in the lumen of the nasal cavity. The induction of apoptosis by loss of cell contact is well described [53], a phenomenon known as anoikis [54] and observed in human airway epithelial cells during SARS-CoV-2 infection [55]. Desquamated cells in the OE may thus be sufficiently preserved to be able to enter apoptosis after the desquamation process is initiated following OE SARS-CoV-2 infection. The C3C-linked apoptosis may also be related to inflammation as well described for SARS-CoV-2 infection [56]. The remaining cells ongoing apoptosis in the lumen may be immune cells as described during SARS-CoV-2 infection [57] and further experiments are required to identify them.

Since we previously observed that the infected area of the OE is infiltrated by immune cells [14], we next explored whether innate immune cells are involved in this process, especially macrophages and neutrophils known to be involved in damage of epithelial cells during acute inflammation [30, 31, 58]. If so, we should systematically observe their presence in the damaged area of the OE. We first characterized the presence of these cells in the infected OE (Fig. 2). We observed that CD68, a classical marker of macrophages [46], was expressed in a different population than $Iba1^+$ cells previously described as a microglia/macrophages cellular population [26]. We observed a continuum of $Iba1^+$ cells staining in the OE and in the olfactory bulb similarly as others [59], indicating that they may be more related to microglia than activated macrophages but they require further phenotyping. In the following, we will thus distinguish $Iba1^+$ cells and macrophages as $CD68^+$ cells to avoid confusion between these two cells types. Immunostaining revealed that at 1 dpi, some parts of the OE in the most rostral part of the nasal cavity were already significantly damaged. We observed that in the infected and damaged area of the OE, $Iba1^+$ cells were mainly recruited while macrophages and neutrophils appeared in the zones desquamating toward the lumen of the nasal cavity. While our qPCR results indicate that neutrophils are recruited more abundantly at 1 dpi than $Iba1^+$ cells and macrophages (Supp. Fig. 3), we observed that contrary to macrophages and neutrophils, $Iba1^+$ cells are already present in the lamina propria of uninfected zones and are rapidly gathering in the infected part of the OE (Fig. 3). The basal presence of $Iba1^+$ cells in the lamina propria could explain the apparent discrepancy between qPCR and immunohistochemistry results. Indeed, at the beginning of infection, the increase of $Iba1^+$ cells could simply arise from infiltration of adjacent cells in the nasal turbinates, while macrophages and neutrophils may migrate from the blood following chemotaxis. We can thus hypothesize that $Iba1^+$ cells are first infiltrating the SARS-CoV-2-infected OE. Similarly, $Iba1^+$ microglia are recruited around infected cells of the central nervous system within hours [27], which is consistent with our observation in the OE. Further studies are required to decipher the origin and specific role of these three cells population during the early events of SARS-CoV-2 infection in the infected nasal turbinates.

Neutrophils are known to induce epithelial damage and an elegant study demonstrated their major role during Poly(I:C) (an artificial double-stranded RNA agonist of TLR3 receptor) nasal instillation leading to damage of the OE [50]. In order to evaluate the importance of the neutrophils in the damage induced by SARS-CoV-2, we first induced neutropenia based on cyclophosphamide treatment successfully used

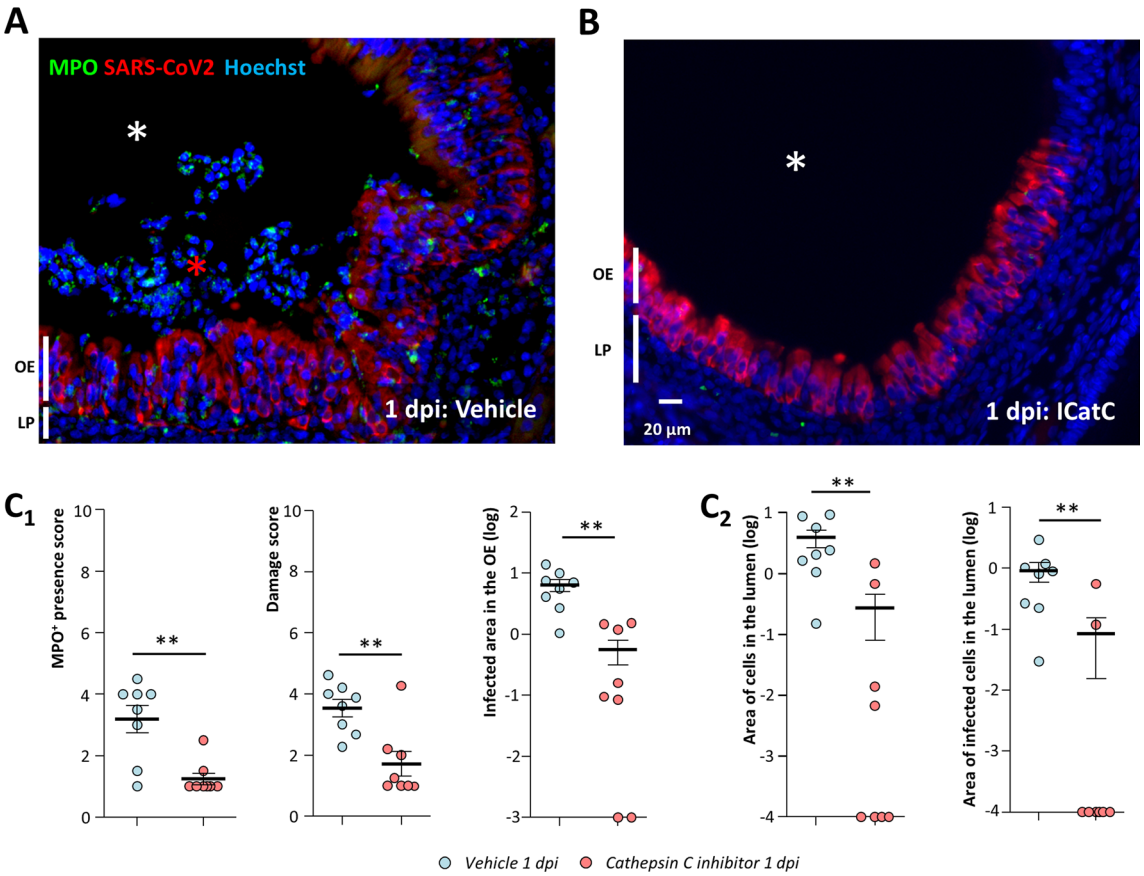

Fig. 6 Inhibition of neutrophil proteinases reduces damage of the olfactory epithelium as well as infected area. Representative images of the infected olfactory epithelium immunostained for MPO (neutrophil marker) and SARS-CoV-2 N protein in (**A**) vehicle and (**B**) cathepsin C inhibitor ($IcatC_{XPZ-01}$) treated animal (olfactory epithelium (OE), lamina propria (LP)). In the vehicle condition, the lumen (white asterisk) is filled with desquamated cells (red asterisk) containing MPO signal. Under cathepsin C inhibition, MPO signal is less abundant and the lumen is mostly free of cellular debris**.** Quantification (**C_1**) in the OE of MPO^+ neutrophil presence; damage score; SARS-CoV-2-infected area and (**C_2**) in the lumen of the nasal cavity of desquamated cell area and percentage of SARS-CoV-2-infected area in the desquamated cells (Mean ± SEM, $n = 8$ areas of the nasal cavity from 4 different animals, $^*p < 0.05$, $^{**}p < 0.01$, $^{***}p < 0.001$ (Mann–Whitney test))

in hamsters [48]. We confirmed that such treatment mainly affects neutrophils but also reduced to a lesser degree other leucocyte populations (Fig. 5A). As expected such treatment reduced neutrophil infiltration in infected areas of the OE and we observed that damage of the infected OE was significantly reduced as well (Fig. $5D_1$, D_2). In order to confirm the role of neutrophils in the damage of the OE following SARS-CoV-2 infection, we treated hamsters with an inhibitor of cathepsin C ($IcatC_{XPZ-01}$) specifically reducing the neutrophil elastase-like proteinases activity [60]. We observed that similar to cyclophosphamide treatment, the damage of the OE was greatly reduced in this context (Fig. $6C_1$). Surprisingly, the global infiltration of neutrophils was reduced as well, even though we observed that some neutrophils were still present in the most infected area of the OE. Since neutrophils are mainly present among the desquamated cells present in the lumen of the nasal cavity, the reduction in neutrophil infiltration during $IcatC_{XPZ-01}$ treatment may be linked to a decrease in the OE damage as elastase-like proteinase action increases inflammation [61]. It suggests that the damage of the OE initiated by neutrophils may participate in the increase in infiltration of neutrophils leading *in fine* to massive damage of the infected OE areas. Additionally, part of the damage of the OE could simply reflect the destruction of sustentacular cells by SARS-CoV-2 as the treatments on neutrophils that we used were not sufficient to completely eliminate neutrophils or their proteases activity. Overall, these results show that neutrophils have a major causative role in the destruction of the OE following SARS-CoV-2 infection by releasing elastase-like proteinases. $Iba1^+$ cells and macrophages seem clearly to be involved as well as they are recruited during the event leading to the damage of the infected OE. Our results with histochemistry show that $Iba1^+$ cells arrive earlier than neutrophils and macrophages.

Iba1$^+$ cells could be involved in the initial events leading to the damage of the OE as well as phagocytosis. However, their importance in the OE damage should be much lower than neutrophils. Indeed, in the CP treatment which did not impact Iba1$^+$ cell presence in the OE at 1 dpi, we still observed a ~ threefold OE damage reduction with only partial inhibition of neutrophils. In the central nervous system, Iba1$^+$ cells are essential to trigger innate immunity response [28]. We can thus hypothesize that Iba1$^+$ cells may play a chemo-attractive role for macrophages and neutrophils in the infected area of the OE. Further experiments are required to decipher their precise importance in the event leading to OE damage following SARS-CoV-2 infection.

We observed that at 1 dpi, the level of SARS-CoV-2 infection was reduced in cyclophosphamide and Icat$C_{XPZ\text{-}01}$-treated hamsters (Figs. 5D_3 and 6C_1). Such a result was unexpected as neutrophils should effectively destroy infected cells and thus their action should reduce infection progression. We observed that these treatments did not impair SARS-CoV-2 replication in the Steno's gland epithelium and in vitro at a dose three times higher than the maximum dose potentially circulating in hamsters during infection (Supp. Fig. 10). As both treatments act on neutrophils, we thus hypothesize that neutrophils damage of the infected OE may have a counterproductive effect by releasing infected cells into the lumen of the nasal cavity. These infected cells could allow the virus to spread more easily in the OE as it was recently observed in human airway epithelial cells during SARS-CoV-2 infection [55]. This process may also be enhanced by the recently demonstrated impairment of mucociliary clearance during SARS-CoV-2 infection [62]. Such a hypothesis is consistent with our results, showing that cyclophosphamide and Icat$C_{XPZ\text{-}01}$ treatment significantly reduced the amount of infected desquamated cells filling the lumen of the nasal cavity (Figs. 5D_4, D_5 and 6C_2). The shedding of SARS-CoV-2 by release of damaged infected cells has been observed recently in vitro in respiratory epithelial cell culture where infection is enhanced in the presence of neutrophils [63]. In this preliminary study, SARS-CoV-2 alone did not significantly increase cytokine production but the neutrophil presence did, showing a major role of the neutrophils in the epithelial response to SARS-CoV-2 infection. In our study, at 2 dpi, the cyclophosphamide treatment inducing neutropenia was less effective than at 1 dpi to prevent OE damage related to SARS-CoV-2 infection (Fig. 5D_2). As the neutropenia was only partial, the remaining neutrophils may be more effectively recruited when infection progresses (Fig. 5D_1) showing the strong ability of SARS-CoV-2 infection in the OE to recruit innate immune cells.

Overall, our results show that the SARS-CoV-2 infection does not directly induce the massive damage of the OE but that neutrophils play a major role by releasing elastase-like proteinase in the infected OE. This probably leads to the destabilization of the OE structures and shedding of infected cells. In the early phase of the infection, the shedding of infected cells could enhance the virus spread in the OE (Fig. 7). We observed damaged areas of the OE as soon as 1

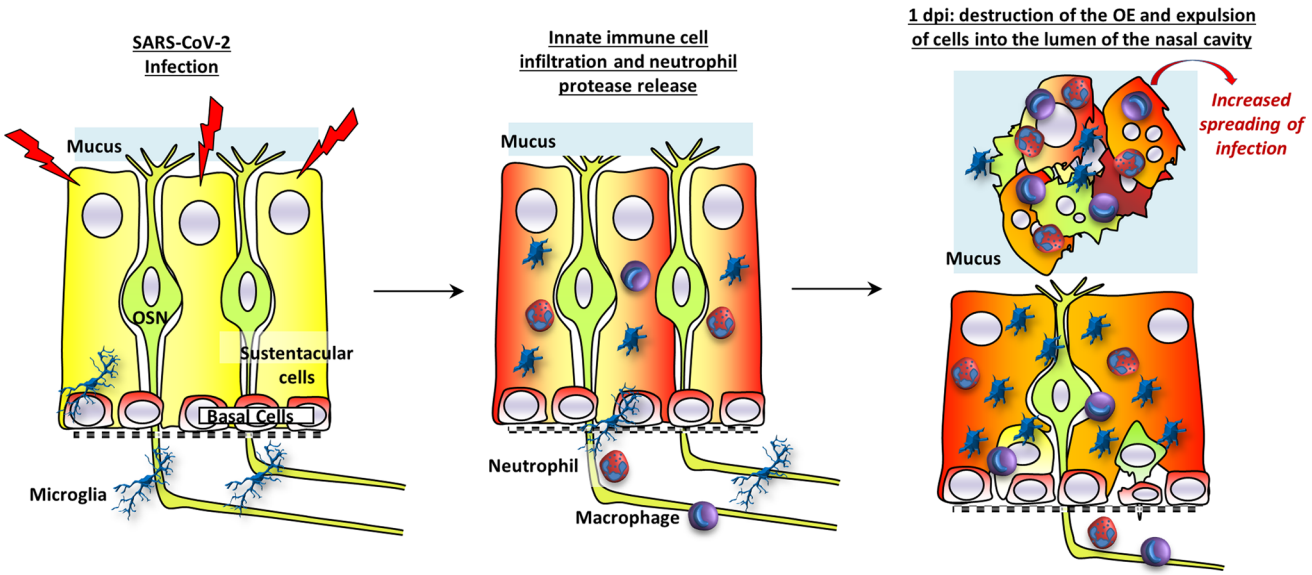

Fig. 7 Model of innate immune cell signaling leading to olfactory epithelium desquamation. The olfactory epithelium is mainly composed of olfactory sensory neurons (OSN) surrounded by supporting cells (sustentacular cells) and basal cells able to regenerate all cell types of the epithelium. During the infection of sustentacular cells (turning red), Iba1$^+$ cells become activated and infiltrate the olfactory epithelium followed by neutrophils and macrophages. Neutrophils release elastase-like proteinase leading to destabilization of the epithelium structures and the expulsion of cells including non-infected neurons into the lumen of the nasal cavity. The release of infected cells may contribute to an increased spreading of the virus in the OE

dpi, indicating that the innate immune system is extremely efficient in detecting SARS-CoV-2-infected cells to destroy them. The signal triggering this very fast action remains to be explored. The host's immune defense system that may be present to prevent pathogen invasion from the nose to the brain seems beneficial for SARS-CoV-2 to achieve a much more extensive infection of the OE than any previous virus, resulting in unprecedented olfactory dysfunction in the COVID-19 pandemic.

Supplementary Information The online version contains supplementary material available at https://doi.org/10.1007/s00018-022-04643-1.

Acknowledgements We would like to thank all VIM members for their helpful discussion, Christopher von Bartheld and Birte Nielsen for improvement of the manuscript, Dr Pierre Deshuillers from the BioPole plateform of the National Veterinary School of Alfort for hamsters' blood count, and all the people from the PRBM platform of ENVA who helped us in the BSL3 animal facility. We would also like to thank Bertrand Bryche, Georges Saade, Mustapha Si-Tahar, Laëtitia Merle and Déborah Diakite for their helpful discussion and technical help.

Author contribution NM and CB were involved in conceptualization; CB, ASA, OAG, BDC, RD, BK, BK, SLP, and NM helped in investigation; CB and NM contributed to formal analysis; NM and CB helped in writing with input from all authors.

Funding NM is supported by INRAe SA department and ANR (Grant CORAR). CB is supported by the "DIM One Health." BK is supported by the "Région Centre Val de Loire (Project Pirana).

Availability of data and material Data will be made available on reasonable request, not applicable for material.

Declarations

Conflict of interest All authors do not have conflict of interest.

Ethics approval and consent to participate Not applicable.

Consent for publication Not applicable.

References

1. Butowt R, Bilińska K, von Bartheld C (2022) Why does the omicron variant largely spare olfactory function? Implications for the pathogenesis of anosmia in COVID-19. J Infect Dis. https://doi.org/10.1093/infdis/jiac113
2. von Bartheld CS, Hagen MM, Butowt R (2020) Prevalence of chemosensory dysfunction in COVID-19 patients: a systematic review and meta-analysis reveals significant ethnic differences. ACS Chem Neurosci. https://doi.org/10.1021/acschemneuro.0c00460
3. Vaira LA, De Vito A, Lechien JR et al (2021) New onset of smell and taste loss are common findings also in patients with symptomatic COVID-19 after complete vaccination. Laryngoscope. https://doi.org/10.1002/lary.29964
4. Boscolo-Rizzo P, Menegaldo A, Fabbris C et al (2021) Six-month psychophysical evaluation of olfactory dysfunction in patients with COVID-19. Chem Senses. https://doi.org/10.1093/chemse/bjab006
5. Lechien JR, Chiesa-Estomba CM, Beckers E et al (2021) Prevalence and 6-month recovery of olfactory dysfunction: a multicentre study of 1363 COVID-19 patients. J Intern Med. https://doi.org/10.1111/joim.13209
6. Renaud M, Thibault C, Le Normand F et al (2021) Clinical outcomes for patients with anosmia 1 year after COVID-19 diagnosis. JAMA Netw Open 4:e2115352. https://doi.org/10.1001/jamanetworkopen.2021.15352
7. Khan AM, Kallogjeri D, Piccirillo JF (2021) Growing public health concern of COVID-19 chronic olfactory dysfunction. JAMA Otolaryngol Head Neck Surg. https://doi.org/10.1001/jamaoto.2021.3379
8. Meunier N, Briand L, Jacquin-Piques A et al (2021) COVID 19-induced smell and taste impairments: putative impact on physiology. Front Physiol. https://doi.org/10.3389/fphys.2020.625110
9. Rebholz H, Braun RJ, Ladage D et al (2020) Loss of olfactory function-early indicator for Covid-19, other viral infections and neurodegenerative disorders. Front Neurol 11:569333. https://doi.org/10.3389/fneur.2020.569333
10. Schwob JE, Jang W, Holbrook EH et al (2017) Stem and progenitor cells of the mammalian olfactory epithelium: taking poietic license. J Comp Neurol 525:1034–1054. https://doi.org/10.1002/cne.24105
11. Bilinska K, Jakubowska P, Bartheld CS, Butowt R (2020) Expression of the SARS-CoV-2 entry proteins, ACE2 and TMPRSS2, in cells of the olfactory epithelium: identification of cell types and trends with age. ACS Chem Neurosci. https://doi.org/10.1021/acschemneuro.0c00210
12. Brann DH, Tsukahara T, Weinreb C et al (2020) Non-neuronal expression of SARS-CoV-2 entry genes in the olfactory system suggests mechanisms underlying COVID-19-associated anosmia. Sci Adv. https://doi.org/10.1126/sciadv.abc5801
13. Fodoulian L, Tuberosa J, Rossier D et al (2020) SARS-CoV-2 receptors and entry genes are expressed in the human olfactory neuroepithelium and brain. iScience. https://doi.org/10.1016/j.isci.2020.101839
14. Bryche B, St Albin A, Murri S et al (2020) Massive transient damage of the olfactory epithelium associated with infection of sustentacular cells by SARS-CoV-2 in golden Syrian hamsters. Brain Behav Immun 89:579–586. https://doi.org/10.1016/j.bbi.2020.06.032
15. Urata S, Kishimoto-Urata M, Kagoya R et al (2021) Prolonged and extended impacts of SARS-CoV-2 on the olfactory neurocircuit. bioRxiv. https://doi.org/10.1101/2021.11.04.467274
16. Storm N, Crossland NA, McKay LGA, Griffiths A (2022) Comparative pathogenicity of SARS-CoV-2 Omicron and Delta variants in Syrian hamsters mirrors the attenuated clinical outlook of Omicron in COVID-19 irrespective of age. Microbiology 24:103530
17. Butowt R, Meunier N, Bryche B, von Bartheld CS (2021) The olfactory nerve is not a likely route to brain infection in COVID-19: a critical review of data from humans and animal models. Acta Neuropathol 141:809–822. https://doi.org/10.1007/s00401-021-02314-2
18. Khan M, Yoo S-J, Clijsters M et al (2021) Visualizing in deceased COVID-19 patients how SARS-CoV-2 attacks the respiratory and olfactory mucosae but spares the olfactory bulb. Cell. https://doi.org/10.1016/j.cell.2021.10.027
19. Seo JS, Yoon SW, Hwang SH et al (2021) The microvillar and solitary chemosensory cells as the novel targets of infection of SARS-CoV-2 in Syrian golden hamsters. Viruses. https://doi.org/10.3390/v13081653
20. Ye Q, Zhou J, He Q et al (2021) SARS-CoV-2 infection in the mouse olfactory system. Cell Discovery 7:49. https://doi.org/10.1038/s41421-021-00290-1

21. Yu P, Deng W, Bao L et al (2022) Comparative pathology of the nasal epithelium in K18-hACE2 Tg mice, hACE2 Tg mice, and hamsters infected with SARS-CoV-2. Vet Pathol. https://doi.org/10.1177/03009858211071016
22. Zhang AJ, Lee AC-Y, Chu H et al (2021) Severe acute respiratory syndrome coronavirus 2 infects and damages the mature and immature olfactory sensory neurons of hamsters. Clin Infect Dis 73:e503–e512. https://doi.org/10.1093/cid/ciaa995
23. Mori I, Goshima F, Imai Y et al (2002) Olfactory receptor neurons prevent dissemination of neurovirulent influenza A virus into the brain by undergoing virus-induced apoptosis. J Gen Virol 83:2109–2116. https://doi.org/10.1099/0022-1317-83-9-2109
24. Le Bon SD, Horoi M (2020) Is anosmia the price to pay in an immune-induced scorched-earth policy against COVID-19? Med Hypotheses 143:109881. https://doi.org/10.1016/j.mehy.2020.109881
25. Burgoyne RA, Fisher AJ, Borthwick LA (2021) The role of epithelial damage in the pulmonary immune response. Cells 10:2763. https://doi.org/10.3390/cells10102763
26. Imai Y, Ibata I, Ito D et al (1996) A novel geneiba1in the major histocompatibility complex class III region encoding an EF hand protein expressed in a monocytic lineage. Biochem Biophys Res Commun 224:855–862. https://doi.org/10.1006/bbrc.1996.1112
27. Fekete R, Cserép C, Lénárt N et al (2018) Microglia control the spread of neurotropic virus infection via P2Y12 signalling and recruit monocytes through P2Y12-independent mechanisms. Acta Neuropathol 136:461–482. https://doi.org/10.1007/s00401-018-1885-0
28. Wheeler DL, Sariol A, Meyerholz DK, Perlman S (2018) Microglia are required for protection against lethal coronavirus encephalitis in mice. J Clin Invest 128:931–943. https://doi.org/10.1172/JCI97229
29. Käufer C, Chhatbar C, Bröer S et al (2018) Chemokine receptors CCR2 and CX3CR1 regulate viral encephalitis-induced hippocampal damage but not seizures. Proc Natl Acad Sci USA 115:E8929–E8938. https://doi.org/10.1073/pnas.1806754115
30. Kolaczkowska E, Kubes P (2013) Neutrophil recruitment and function in health and inflammation. Nat Rev Immunol 13:159–175. https://doi.org/10.1038/nri3399
31. Meidaninikjeh S, Sabouni N, Marzouni HZ et al (2021) Monocytes and macrophages in COVID-19: friends and foes. Life Sci 269:119010. https://doi.org/10.1016/j.lfs.2020.119010
32. Janoff A (1972) Human granulocyte elastase. Further delineation of its role in connective tissue damage. Am J Pathol 68:579–592
33. Kawabata K, Hagio T, Matsuoka S (2002) The role of neutrophil elastase in acute lung injury. Eur J Pharmacol 451:1–10. https://doi.org/10.1016/S0014-2999(02)02182-9
34. Brinkmann V, Reichard U, Goosmann C et al (2004) Neutrophil extracellular traps kill bacteria. Science 303:1532–1535. https://doi.org/10.1126/science.1092385
35. Saffarzadeh M, Juenemann C, Queisser MA et al (2012) Neutrophil extracellular traps directly induce epithelial and endothelial cell death: a predominant role of histones. PLoS ONE 7:e32366. https://doi.org/10.1371/journal.pone.0032366
36. Arango Duque G, Descoteaux A (2014) Macrophage cytokines: involvement in immunity and infectious diseases. Front Immunol. https://doi.org/10.3389/fimmu.2014.00491
37. Borders AS, Getchell ML, Etscheidt JT et al (2007) Macrophage depletion in the murine olfactory epithelium leads to increased neuronal death and decreased neurogenesis. J Comp Neurol 501:206–218. https://doi.org/10.1002/cne.21252
38. Borders AS, Hersh MA, Getchell ML et al (2007) Macrophage-mediated neuroprotection and neurogenesis in the olfactory epithelium. Physiol Genomics 31:531–543. https://doi.org/10.1152/physiolgenomics.00008.2007
39. Hoagland DA, Moller R, Uhl SA et al (2021) Leveraging the antiviral type I interferon system as a first line of defense against SARS-CoV-2 pathogenicity. Immunity. https://doi.org/10.1016/j.immuni.2021.01.017
40. Korkmaz B, Lesner A, Wysocka M et al (2019) Structure-based design and in vivo anti-arthritic activity evaluation of a potent dipeptidyl cyclopropyl nitrile inhibitor of cathepsin C. Biochem Pharmacol 164:349–367. https://doi.org/10.1016/j.bcp.2019.04.006
41. Guarino C, Hamon Y, Croix C et al (2017) Prolonged pharmacological inhibition of cathepsin C results in elimination of neutrophil serine proteases. Biochem Pharmacol 131:52–67. https://doi.org/10.1016/j.bcp.2017.02.009
42. Bryche B, Dewaele A, Saint-Albin A et al (2019) IL-17c is involved in olfactory mucosa responses to Poly(I:C) mimicking virus presence. Brain Behav Immun. https://doi.org/10.1016/j.bbi.2019.02.012
43. Bryche B, Fretaud M, Saint-Albin Deliot A et al (2019) Respiratory syncytial virus tropism for olfactory sensory neurons in mice. J Neurochem. https://doi.org/10.1111/jnc.14936
44. Muller PY, Janovjak H, Miserez AR, Dobbie Z (2002) Processing of gene expression data generated by quantitative real-time RT-PCR. Biotechniques 32:1372–1374 (**1376, 1378–1379**)
45. Bouchery T, Harris N (2019) Neutrophil–macrophage cooperation and its impact on tissue repair. Immunol Cell Biol 97:289–298. https://doi.org/10.1111/imcb.12241
46. Holness C, Simmons D (1993) Molecular cloning of CD68, a human macrophage marker related to lysosomal glycoproteins. Blood 81:1607–1613. https://doi.org/10.1182/blood.V81.6.1607.1607
47. Leto TL, Lomax KJ, Volpp BD et al (1990) Cloning of a 67-kD neutrophil oxidase factor with similarity to a noncatalytic region of p60 $^{c\text{-}}$src. Science 248:727–730. https://doi.org/10.1126/science.1692159
48. Peniche AG, Bonilla DL, Palma GI et al (2017) A secondary wave of neutrophil infiltration causes necrosis and ulceration in lesions of experimental American cutaneous leishmaniasis. PLoS ONE 12:e0179084. https://doi.org/10.1371/journal.pone.0179084
49. Borregaard N, Theilgaard-Mönch K, Sørensen OE, Cowland JB (2001) Regulation of human neutrophil granule protein expression. Curr Opin Hematol 8:23–27. https://doi.org/10.1097/00062752-200101000-00005
50. Kanaya K, Kondo K, Suzukawa K et al (2014) Innate immune responses and neuroepithelial degeneration and regeneration in the mouse olfactory mucosa induced by intranasal administration of Poly(I:C). Cell Tissue Res 357:279–299. https://doi.org/10.1007/s00441-014-1848-2
51. Fumagalli V, Ravà M, Marotta D et al (2022) Administration of aerosolized SARS-CoV-2 to K18-hACE2 mice uncouples respiratory infection from fatal neuroinvasion. Sci Immunol 7:eabl9929. https://doi.org/10.1126/sciimmunol.abl9929
52. Raynaud A, Meunier N, Acquistapace A, Bombail V (2015) Chronic variable stress exposure in male Wistar rats affects the first step of olfactory detection. Behav Brain Res 291:36–45. https://doi.org/10.1016/j.bbr.2015.05.013
53. Bates RC, Buret A, van Helden DF et al (1994) Apoptosis induced by inhibition of intercellular contact. J Cell Biol 125:403–415. https://doi.org/10.1083/jcb.125.2.403
54. Frisch S, Francis H (1994) Disruption of epithelial cell-matrix interactions induces apoptosis. J Cell Biol 124:619–626. https://doi.org/10.1083/jcb.124.4.619
55. Morrison CB, Edwards CE, Shaffer KM et al (2022) SARS-CoV-2 infection of airway cells causes intense viral and cell shedding, two spreading mechanisms affected by IL-13. Proc Natl Acad Sci USA 119:e2119680119. https://doi.org/10.1073/pnas.2119680119

56. Li S, Zhang Y, Guan Z et al (2020) SARS-CoV-2 triggers inflammatory responses and cell death through caspase-8 activation. Sig Transduct Target Ther 5:235. https://doi.org/10.1038/s41392-020-00334-0
57. Junqueira C, Crespo Â, Ranjbar S et al (2022) FcγR-mediated SARS-CoV-2 infection of monocytes activates inflammation. Nature. https://doi.org/10.1038/s41586-022-04702-4
58. Hasegawa-Ishii S, Shimada A, Imamura F (2017) Lipopolysaccharide-initiated persistent rhinitis causes gliosis and synaptic loss in the olfactory bulb. Sci Rep 7:11605. https://doi.org/10.1038/s41598-017-10229-w
59. Ueha R, Ito T, Furukawa R et al (2022) Oral SARS-CoV-2 inoculation causes nasal viral infection leading to olfactory bulb infection: an experimental study. Front Cell Infect Microbiol 12:924725. https://doi.org/10.3389/fcimb.2022.924725
60. Guarino C, Legowska M, Epinette C et al (2014) New selective peptidyl di(chlorophenyl) phosphonate esters for visualizing and blocking neutrophil proteinase 3 in human diseases. J Biol Chem 289:31777–31791. https://doi.org/10.1074/jbc.M114.591339
61. Döring G (1994) The role of neutrophil elastase in chronic inflammation. Am J Respir Crit Care Med 150:S114–S117. https://doi.org/10.1164/ajrccm/150.6_Pt_2.S114
62. Li Q, Vijaykumar K, Philips SE et al (2022) Mucociliary transport deficiency and disease progression in Syrian hamsters with SARS-CoV-2 infection. Microbiology 5:562
63. Calvert B, Quiroz E, Lorenzana Z et al (2021) Neutrophilic inflammation promotes SARS-CoV-2 infectivity and augments the inflammatory responses in airway epithelial cells. https://doi.org/10.1101/2021.08.09.455472